

# Analysing Carbon Deposition on Ni/YSZ Anode Tested in an Solid Oxide Fuel Cell (SOFC)

G. Almutairi, Y. Alyousef and F. Alenazey

Water and Energy Research Institute, King Abdulaziz City for Science and Technology (KACST),  
PO. Box. 6086, Riyadh 11442, Saudi Arabia

Received: June 12, 2017, Accepted: July 19, 2017, Available online: July 28, 2017

**Abstract:** Integrated Planar Solid Oxide Fuel Cells (IP-SOFC), which utilise a Ni/YSZ based anode, have been operated under direct hydrogen-methane mixture fuel injection at 900 °C. This process has shown some disadvantages in fuelling to the IP-SOFC; producing carbon deposition from the methane in the fuel mixture, causing direct structural damage to the IP-SOFC surface and blocking the area of activation for reaction processes and reducing the performances. These factors were shown to adversely affect the performance of the IP-SOFC over time. The aim of this paper is to calculate the amount of carbon deposited through the use of temperature programmed oxidation (TPO). In addition, the distribution of carbon is studied and analysed on all parts of the IP-SOFC cells. The results show that both amorphous and graphitic carbon were formed causing microstructural damage thereby reducing the cell performance. Furthermore, the reaction temperature was demonstrated to increase the total amount of carbon deposition.

**Keywords:** IP-SOFC, degradation, carbon deposition, temperature programmed oxidation

## 1. INTRODUCTION

Solid oxide fuel cells (SOFCs) are electrochemical reactors that can efficiently convert fuel gas chemical energy into electrical energy with minimal environmental hazards [1,2]. Current studies of solid oxide fuel cells focus on the available hydrocarbon fuels usage. Ni/YSZ cermet is the most commonly used anode material, but it possesses some disadvantages when hydrocarbons are used as fuels. Therefore, there is a need to develop alternative anode materials that are capable of displaying mixed conductivity when subjected to complex fuels [3].

Cells with Ni/YSZ anode have two main problems when using fuels such as natural gas. These problems are impurity poisoning and carbon deposition. Impurity poisoning, such as phosphide, chloride, or sulphide, damages the solid oxide fuel cell (SOFC) anode leading to fast degradation [4,5]. Carbon deposition occurs due to the fact that Ni is an excellent catalyst for these kinds of reactions, such as methane cracking (equation 1), reduction of carbon monoxide (equation 2) and disproportionation of monoxide (equation 3). Therefore, Ni catalysts can be deactivated by the carbon deposited, resulting in rapid cell degradation [6].



Various strategies have been devised to limit carbon deposition in SOFCs. Studies conducted on the direct oxidation of natural gas indicate that the carbon deposition on a nickel/yttrium-stabilized zirconia (Ni/YSZ) anode can be prevented by increasing the operation current density and lowering the operation temperature [7,8]. However, these two operation parameters are not easily attainable in real SOFC systems. Another strategy, which has been used to prevent carbon deposition in the internal steam reforming of natural gas, by using a high steam to carbon ratio (S/C). This strategy dilutes the fuel, however, resulting in the reduction of cell electrical efficiency [9,10].

Different carbon species exist and their deposition varies depending on the reaction conditions. One of the species of carbon is referred to as carbidic (C bonded to Ni). The carbidic species are formed at temperatures equal to or below 350 °C, and hence are not normally observed in SOFCs. The second carbon species is referred to as adsorbed or amorphous carbon, which forms at temperatures above 350 °C. This material is referred to as graphitic

\*To whom correspondence should be addressed: Email: gmotari@kacst.edu.sa  
Phone: 966 (0) 11481 3905



Figure 1. Integrated Planar Solid Oxide Fuel Cell (IP-SOFC).

layers which are formed above 450 °C. Graphitic layers and adsorbed carbon are easily deposited in hydrocarbon-fuelled SOFCs [6].

In order to resolve the problem of carbon deposition, Ni/YSZ has been replaced by many anode materials such as gadolinium doped ceria, doped SrTiO<sub>3</sub> [11,12] and Cu-CeO-YSZ [13]. Nonetheless, these substitute materials possess some disadvantages, such as complicated fabrication processes, low conductivity or poor electrochemical catalyst activity. This leaves Ni/YSZ cermet as the most preferred anode material. Hence, it is crucial to understand and control carbon deposition behaviour on the Ni/YSZ anode.

Carbon deposition can be decreased by increasing the current density, and it can be even become zero at a critical current density [14]. Steam supplied in the feed stream was also shown to decrease the amount of carbon deposition through the study conducted by Laycock, Staniforth and Ormerod [15]. Increases in temperature in the study it caused the amount of carbon to decrease at first and then increase.

The research on carbon deposition in SOFCs with a Ni-based anode commonly focuses on three critical issues. The first is thermodynamic calculation, which assists in predicting the carbon deposition conditions. However, such calculations are likely to deviate from real situations and necessitate experimental verification. Some experimental studies on thermodynamic calculation, such as direct oxidation and the internal reforming of methane, have been carried out for certain fuels. The second issue is species of the deposited carbon. Several studies have indicated that the carbon morphologies and species depend on the operation of reactants and temperature [6, 16-17]. Using the technology of temperature-programmed oxidation (TPO) and temperature-programmed reduction (TPR) help to identify the carbon species which are produced from methane cracking as reported by Finnerty et al [18].

This paper describes the on going investigations through the identification of characteristics of the carbon species and by calculating the amount of carbon through the use of temperature programmed oxidation (TPO). In addition, the distribution of carbon is studied and analysed on all parts of the IP-SOFC cells, to build upon the understanding of these processes and develop this technology further.

## 2. EXPERIMENTAL

### 2.1. IP-SOFC tube

The IP-SOFC utilized in this project operates in the same way as



Figure 2. The IP-SOFC piece inside a quartz tube in furnace.

a standard SOFC that employs natural gas (methane) or hydrogen as fuel. The design of the IP-SOFC is based on a rectangular flat porous ceramic tube which supplies fuel to the anode. The tube is screen printed with anode (Ni/YSZ based), cathode (LSM-based), electrolyte (YSZ-based) and interconnected layers (LCC). Each tube comprises 30 cell pairs connected in series, each with a cell area of 6 cm<sup>2</sup> [19-20], as illustrated in Figure 1. After long term testing with operation under direct hydrogen-methane mixture fuel injection at 900 °C, the cell numbers 5, 10, 15, 20, 25, and 29 of IP-SOFC were then cut to two pieces. One piece was used as the top cell and second piece as the bottom cell. The surface area of one such piece was around 3 cm<sup>2</sup>.

### 2.2. Testing procedure

The temperature-programmed oxidation (TPO) experiment was completed by packing the IP-SOFC pieces inside a quartz glass tube reactor, which was then put into a furnace, as shown in Figure 2.

Here, the TPO process was used to study the formation of carbon deposition on the anode surface. TPO was applied by using a constant flow of helium (20 millilitres per minute) and oxygen (5 millilitres per minute) into the quartz tube, which contained small pieces of the IP-SOFC tube. The furnace was then heated to 850 °C at a rate of 10°C per minute. The outlet of the quartz tube was connected to an on-line mass spectrometer to evaluate the exhaust gases. The peak of CO<sub>2</sub> and CO measured on the mass spectrometer trace was used to quantify the formation of carbon deposition.

CABOT carbon black was used to calibrate the amount of deposition of carbon. Varying amounts of carbon black were exposed to oxygen to form carbon dioxide and carbon monoxide. Variations in the amount of carbon black was analysed by using the TPO technique where known amounts of carbon black gives a relationship between the area under the CO and CO<sub>2</sub> peaks and the amount of carbon oxidised.

## 3. RESULTS AND DISCUSSION

Figure 3 shows the average voltage output of the IP-SOFC at constant current (1.0A), which includes three stages: Run 1 and

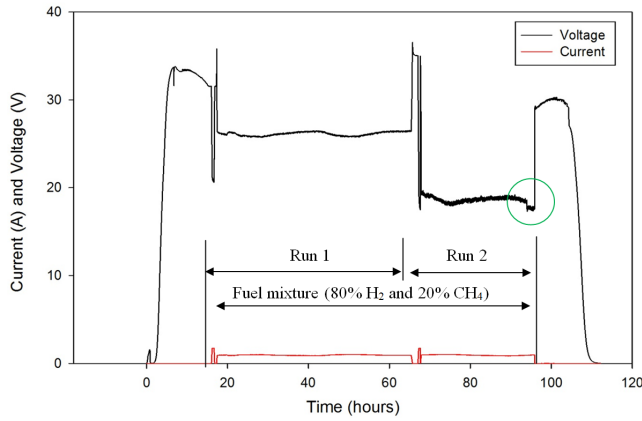


Figure 3. Second durability test operated with 80% H<sub>2</sub> and 20% CH<sub>4</sub>.

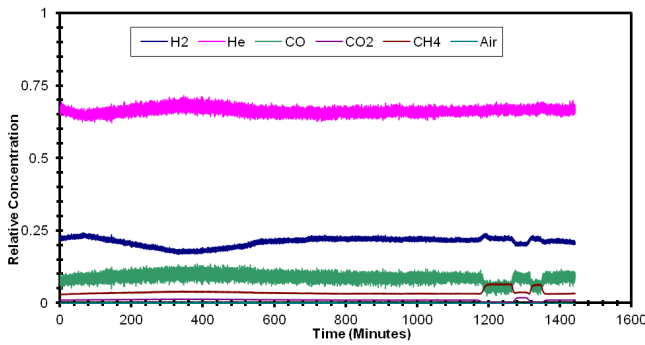


Figure 4. Exhaust gas analysis for helium and fuel mixture at 900°C.

Run 2 with a fuel mixture (80% H<sub>2</sub> and 20% CH<sub>4</sub>) and the final stage IP-SOFC with pure hydrogen for a short time (around 5 hours) (shown by a green circle). The difference between the three stages became clear when IP-SOFC started losing considerable amounts of voltage. Comparison of the three stages for operating IP-SOFC, shows that Run 1 gave the best average voltage, where the voltage output of the IP-SOFC was around 25.7 V at constant current (1.0A) for a period 48 hours. Following this, the IV curve was recorded then Run 2 was started, where the average voltage was shown to decline significantly. The voltage decreased from 25.7 V to 18.48 V at a constant current (1.0A) in Run 1 and Run 2 respectively. The fuel was then changed to pure hydrogen and a decline of 1.0V at constant current was also recorded (1.0A).

There are many reactions that are likely to occur with the passing of oxygen ions through the electrolyte [22]. The methane gas reacts with oxygen ions to produce water, carbon monoxide and carbon dioxide, as shown in the following equations:

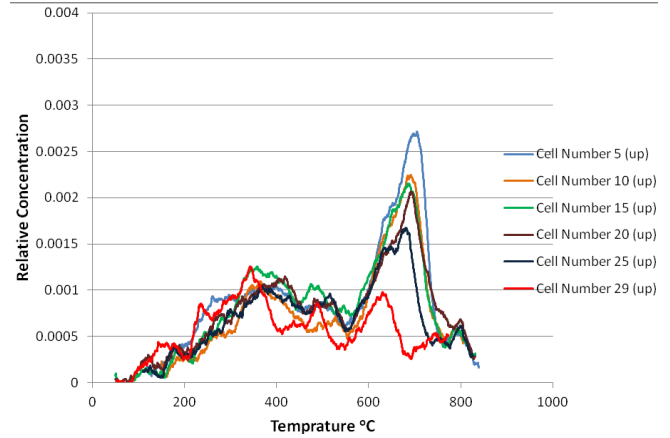
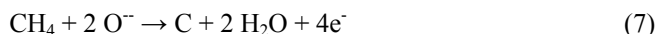
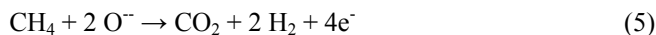
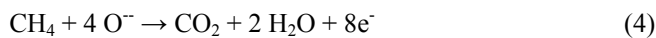


Figure 5. TPO spectra of CO<sub>2</sub> for top part of IP-SOFC cells.

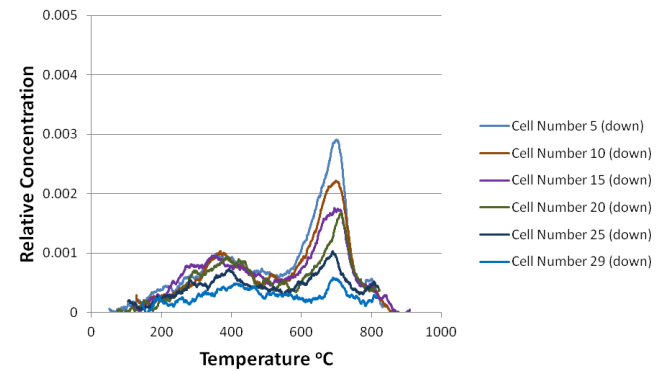


Figure 6. TPO spectra of CO<sub>2</sub> for bottom part of IP-SOFC cells.

It is clear from Figure 4 that the exhaust gas analysis result shows that it contains hydrogen, carbon monoxide, methane and very little carbon dioxide, where the methane gas produces carbon monoxide and carbon dioxide.

It is also likely to produce carbon leading to carbon deposition. The peak of carbon dioxide emission produced was measured by the mass spectrometer for all of the cells. Figure 5 shows the TPO spectra of CO<sub>2</sub> for the top part of the IP-SOFC cells, whereas Figure 6 shows the TPO spectra of CO<sub>2</sub> produced for the bottom part of the IP-SOFC cells. In both of these Figures, two peaks were evident at temperatures between 150 and 550 °C, and between 550 and 780 °C, which represents two types of carbon. The first one is known as amorphous carbon, peaking in the range of ~350 to ~430 °C and the second is known as graphitic carbon, peaking between ~650 and ~750 °C. From these peaks the mass of carbon on the surface of the IP-SOFC can be calculated. These different carbon types and their deposition vary depending on the reaction temperature.

The areas under the peaks between 550 °C and 780 °C in Figure 5 and the graphitic regions in Figure 6 were calculated using the Trapezoidal rule. The amount of carbon deposition was calculated for both top and bottom of IP-SOFC regions, where the surface areas of each sample differ from the surface area of other samples, the amount of carbon deposition is divided by the area of sample to

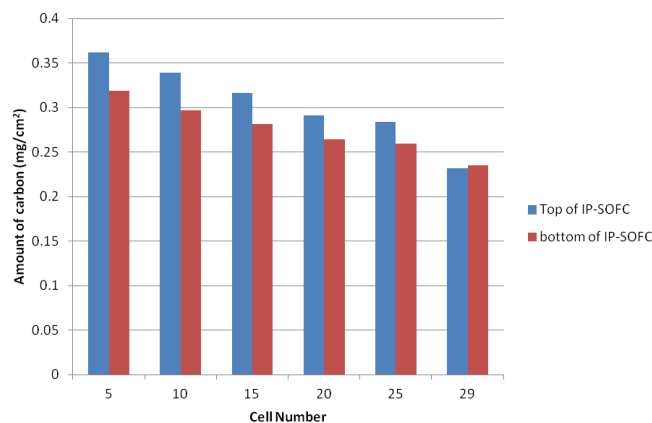


Figure 7. Histogram of the weight of carbon deposition in cells 5, 10, 15, 20, 25 and 29.

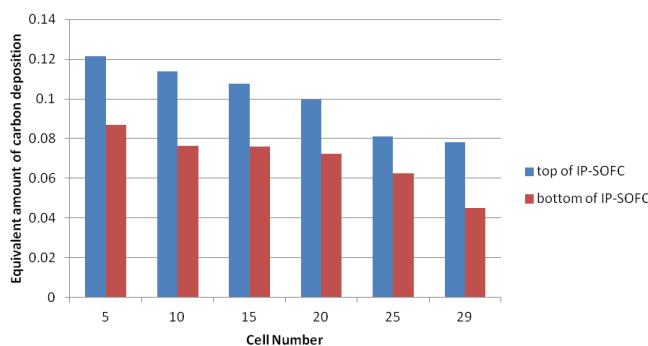


Figure 8. The equivalent amount of amorphous carbon deposited in cells.

calculate it in  $\text{cm}^2$  to facilitate comparison with other samples.

Using the results of these calculations, the total amount of carbon deposition in cells 5, 10, 15, 20, 25 and 29 for the top and bottom region of IP-SOFC is plotted in Figure 7.

It is apparent in Figure 7 that the largest amount of graphitic carbon deposition is found in the beginning of the cells of the IP-SOFC. For the top cells, the total amount of carbon was  $369 \mu\text{g per cm}^2$  at cell number 5. Carbon deposition then gradually decreases, to the level where the total amount of carbon was  $231 \mu\text{g per cm}^2$  at the top of cell number 29. Similarly, in the bottom cells, the total amount of carbon decreases from  $319 \mu\text{g per cm}^2$  in cell 5 to  $235 \mu\text{g per cm}^2$  in cell 29.

The second type is amorphous carbon, which oxidises at approximately  $300 \text{ }^\circ\text{C}$ , as shown in Figure 5 (top of the IP-SOFC) and Figure 6 (bottom of the IP-SOFC). From these Figures the area under curves (between  $150$  and  $550 \text{ }^\circ\text{C}$ ) was calculated by the Trapezoidal rule to deduce the amorphous carbon deposited on the anode surface of the IP-SOFC.

Using the data from calculations, the total equivalent amount of carbon deposition in cells 5, 10, 15, 20, 25 and 29 at top and bottom regions of the IP-SOFC for amorphous carbon is shown in Figure 8.

As shown in Figure 8, the largest amount of amorphous carbon

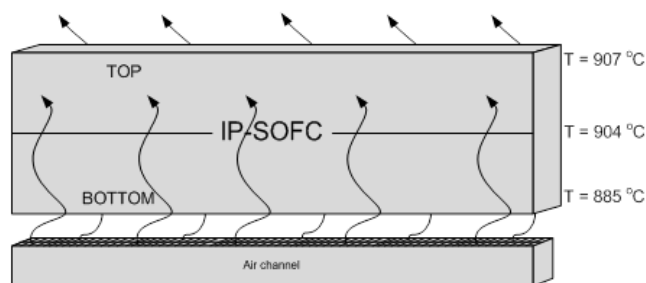


Figure 9. A schematic diagram of the distribution of temperature across the IP-SOFC.



Figure 10. Cracking in the surface cells of the IP-SOFC.

deposition occurs at the beginning of the top cells of the IP-SOFC. The total equivalent amount of amorphous carbon was  $0.121 \text{ per cm}^2$  at the top of cell number 5. This gradually decreases to the point where the total amount of amorphous carbon was  $0.0783 \text{ per cm}^2$  at the top of cell number 29. The total equivalent amount of amorphous carbon also decreases at the bottom of the IP-SOFC from  $0.0870 \text{ per cm}^2$  at cell number 5 to  $0.0448 \text{ per cm}^2$  at cell number 29.

The difference in the total amount of carbon deposition (graphitic carbon) in the cells of the IP-SOFC, depending on many parameters such as methane consumption and reaction temperature, where the amount of methane was consumed along the gas channels in the IP-SOFC.

The second parameter that affects the total amount of carbon was reaction temperature. As a result, air was pumped from the bottom of the IP-SOFC surrounding the cells and the temperature entering was less than the temperature of the furnace as shown in Figure 9. This causes variation in the temperature of the IP-SOFC.

The variation in the total amount of carbon with reaction temperature was significant. Carbon deposition increased with increasing reaction temperature due to methane decomposition, becoming both kinetically and thermodynamically favourable with increasing reaction temperature. As can be seen in Figure 7 and Figure 8, the total carbon deposition in the bottom region was lower than in the top region for all the cells of the IP-SOFC. At the top of cell number 5, the total amount of carbon was  $369 \mu\text{g per cm}^2$  at the average of temperature of  $907 \text{ }^\circ\text{C}$ , whereas at the bottom of the same cell, the total amount of carbon was  $319 \mu\text{g per cm}^2$  at the average temperature of  $885 \text{ }^\circ\text{C}$ . Over the whole of the IP-SOFC the largest

amount of carbon deposition was recorded in the top region that was exposed to the highest reaction temperature.

It can be noted that the degradation rate in the SOFC is low, which is < 1% per 1000 hours operated for industrial application. Carbon deposition was the most important factor influencing the stability in a solid oxide fuel cell operating with fuel containing hydrocarbons such as methane, potentially causing fast degradation in the performance [6].

The IP-SOFC features a porous ceramic support, which is a very hard layer and an anode layer printed above this, which contains nickel material. Ni is an excellent catalyst for carbon deposition reactions. In this case, the carbon forms between the porous ceramic support and the anode layer, leading to cracking of the cells of the IP-SOFC layer as shown in Figure 10, causing the damage to the cell.

#### 4. CONCLUSION

The following conclusions were drawn from the present investigation:

- The IP-SOFC porous ceramic support was operated successfully under a fuel mixture (hydrogen and methane) to study the degradation behaviour of the IP-SOFC caused due to carbon deposition at operating temperature of 900 °C.
- Carbon was formed on the anode surface when operating the cells using a H<sub>2</sub> and CH<sub>4</sub> fuel mixture at 900 °C. Two types of carbons have been found to be deposited: amorphous carbon, which oxidises between 150 °C and 550 °C, and graphitic carbon, which oxidises between 550 °C and 780 °C.
- Two key parameters affect the increase in the total amount of carbon deposition on the anode surface of the IP-SOFC: these are reaction temperature and methane consumption.
- Carbon deposition is an important factor in IP-SOFC degradation, leading to direct structural damage of the IP-SOFC surface, which is composed of carbon between a porous ceramic support and an anode layer.

#### REFERENCES

- [1] T. Komatsu, K. Watanabe, M. Arakawa, H. Arai., Journal of Power Sources, 193, 585 (2009).
- [2] K. Kevin, Q. Nguyen, C. S. Singhal, High Temperature Solid Oxide Fuel Cells: Fundamentals, Design and Applications. Cell Stack and Designs, Elsevier Ltd., Oxford 2003, pp. 197–228.
- [3] C. Sun, U. Stimming, Journal of Power Sources, 171, 247 (2007).
- [4] F. N. Cayan, M. Zhi, S. R. Pakalapati, I. Celik, N. Wu, R. Gemen , Journal of Power Sources, 185, 595 (2008).
- [5] T. S. Li, H. Miao, T. Chen, W. G. Wang, C. Xuz, Journal of The Electrochemical Society, 156, B1383 (2009).
- [6] T. Chen, W. G. Wang, H. Miao, T. Li, C. Xu, Journal of Power Sources, 196, 2461 (2011).
- [7] Y. Lin, Z. Zhan, J. Liu, S. A. Barnett, Solid State Ionics, 176, 1827 (2005).
- [8] J. Liu, S.A. Barnett, Solid State Ionics, 158, 11 (2003).
- [9] A. Gunji, C. Wen, J. Otomo, T. Kobayashi, K. Ukai, Y. Mizutani, H. Takahash, Journal of Power Sources, 131, 285 (2004).
- [10] P. Vernoux, M. Guillo, J. Foulletier, A. Hammou, Solid State Ionics, 135, 425 (2000).
- [11] J. Canales-Vazquez, S.W. Tao, J.T.S. Irvine, Solid State Ionics, 159, 159 (2003).
- [12] S. Hui, A. Petric, Journal of The Electrochemical Society, 149, J1 (2002).
- [13] S. Park, J.M. Vohs, R.J. Gorte, Nature, 404, 265 (2000).
- [14] D. Singh, E. Hernandez-Pacheco, P. N. Hutton, N. Patel, M. D. Mann, Journal of Power Sources, 142, 194 (2005).
- [15] C.J. Laycock, J.Z. Staniforth, R.M. Ormerod, Dalton Transactions, 40, 5494 (2011).
- [16] A. Dhir, K. Kendall, Journal of Power Sources, 181, 297 (2008).
- [17] G. Almutairi, A. Dhir, W. Bujalski, Fuel Cells, 2014, in press.
- [18] C. M. Finnerty, N. J. Coe, R. H. Cunningham, R. M. Ormerod, Catalysis Today, 46, 137 (1998).
- [19] F.J. Gardner, M.J. Day, N.P. Brandon, M.N. Pashley, M. Cassidy, Journal of Power Sources, 86, 122 (2000).
- [20] A. Spangler, G. Agnew, 9th Grove Fuel Cell Symposium. 2005: London, UK.
- [21] G. Almutairi, K. Kendall and W. Bujalski, Cycling durability studies of IP-SOFC, International Journal of Low-Carbon Technologies, 7, 63 (2012).
- [22] C. Mallon, in Chemical Engineering. 2006, The University of Birmingham: Birmingham.